

SPONTANEOUS SYMMETRY BREAKING AND PROPER-TIME FLOW EQUATIONS

Alfio Bonanno

INAF - Osservatorio Astrofisico, Via S.Sofia 78, I-95123 Catania, Italy
INFN Sezione di Catania, Via S.Sofia 64, I-95123 Catania, Italy

Giuseppe Lacagnina

Institut für Theoretische Physik, Universität Regensburg,
D-93040 Regensburg, Germany

Abstract

We discuss the phenomenon of spontaneous symmetry breaking by means of a class of non-perturbative renormalization group flow equations which employ a regulating smearing function in the proper-time integration. We show, both analytically and numerically, that the convexity property of the renormalized local potential is obtained by means of the integration of arbitrarily low momenta in the flow equation. Hybrid Monte Carlo simulations are performed to compare the lattice Effective Potential with the numerical solution of the renormalization group flow equation. We find very good agreement both in the strong and in the weak coupling regime.

1 Introduction

The mechanism of spontaneous symmetry breaking is one of the most important nonperturbative phenomena in quantum field theory and statistical mechanics. Unfortunately, due to its strong nonperturbative character, many of its aspects are not yet well understood mainly because of the lack of reliable computational tools even in simple physical situations. For example, in the liquid-vapor phase transition, the system undergoes a first-order phase transition below the critical temperature, but the presence of long-range fluctuations renders the mean-field description inadequate. The well-known Maxwell construction [1] reproduces the flat isotherms in the two-phase region but does not provide the correct critical exponents near the critical region.

In quantum field theory the situation is even more dramatic because the perturbative calculation of the Effective Potential (EP) generates an imaginary part whose physical meaning is not entirely clear. In fact, the EP should be a convex function of the fields by construction, since it is the Legendre transform of the generating functional of the connected Green's functions [2].

An important result was obtained in [3] within the framework of the Effective Average Action, for a continuous $O(N)$ -symmetric scalar theory: it was shown that in order to correctly reproduce the convexity property of the free energy a non-trivial saddle point (spin wave solution) must be chosen in the loop-expansion [4]. This result has opened the possibility of using the Wilsonian RG approach in discussing non-perturbative issues of this kind.

Quite generally the possibility of applying renormalization group (RG) methods to the description of first order phase transition has frequently been matter of discussion in the recent years. Although the question is still not completely settled, several works have shown that the Wilsonian RG approach is a promising tool for such kind of investigations. In particular it has been shown [5] that the Wegner-Houghton (WH) RG equation (a sharp cut-off momentum-space wilsonian-type of RG flow equation) already in the simple local potential approximation (LPA) reproduces the convexity property of the free energy as a result of the integration of arbitrarily low momenta without resorting to any *ad hoc* Maxwell construction, or saddle point approximation. Moreover, the RG transformation is always well defined below the critical line.

The essential ingredient of their analysis was the use of a robust and very accurate numerical method for handling the RG equation without resorting to polynomial truncations. Similar results have also been obtained with a smooth cutoff RG flow equation, in the framework of the exact RG equation for the effective average action [6]. In [7] an alternative method which combines the RG flow equation approach with the non-trivial saddle point expansion method has been presented.

The wilsonian RG transformation [9], as opposed to the more conventional RG transformation based on the rescaling properties of the Green's functions, preserves all the infinite number of interactions generated in the low-energy action by “averaging-out” the small-scale physics defined at some high-energy scale Λ , and for this reason is a powerful tool in order to investigate situations where infinitely many length scales are coupled together. Quite generally, the Wilsonian action can be defined as

$$e^{-S_\Omega(\Phi)} = \int \mathcal{D}\varphi \delta(\Phi - C(\varphi)) e^{-S(\varphi)} \quad (1.1)$$

where Φ is a low frequency field which is in turn a function of the fundamental field φ via $\Phi = C(\varphi)$ and C is some averaging operator. If the effective theory is defined on a lattice Λ_0 , then

$$\delta(\Phi - C(\varphi)) = \prod_{x \in \Lambda_0} \delta(\Phi(x) - C(\varphi)(x))$$

For computational purposes, a continuous wilsonian RG transformation is defined in the momentum-space representation where the definition (1.1) becomes

$$e^{-S_k(\Phi)} = \int \mathcal{D}\zeta e^{-S(\zeta + \Phi)} \quad (1.2)$$

ζ being the high-frequency part of the fundamental field with momenta p greater than some infrared cutoff $p > k$, and Φ the low-frequency one, with momenta $p \leq k$. If we choose

$$C(\varphi) = \frac{1}{\Omega} \int_{\Omega} \varphi \quad (1.3)$$

where Ω is a characteristic volume over which the field is averaged, in the limit $\Omega \rightarrow \infty$ (equivalently, vanishing infrared cutoff k in Eq.(1.2)) the blocked action gives precisely the EP, namely the non-derivative part of the Effective Action $\Gamma[\phi]$, defined as the Legendre transform of $W[J]$, the generator of the connected Green's functions in the presence of an external current J [8].

In practice, the wilsonian RG transformation obtained from explicit calculation of (1.2) is strongly non-linear, and only by retaining infinitely many interactions generated by integrating out the “fast” variable, the RG transformation can be well defined below the critical line. Therefore, a numerical treatment of the full non-linear partial differential equation is necessary even in the simplest LPA approximation of the Wilsonian Action.

In recent years, in an attempt of calculating (1.2) non-perturbatively, a new type of RG flow equations has been proposed [?] and further developed [10, 11, 12]. It is based on Schwinger’s proper time regulator, and it is therefore well suited for a direct application to gauge theories.

The proper time renormalization group equation (PTRG) does not belong to the class of exact-RG flows which can be formally derived from the Green’s functions generator without resorting to any truncation or approximation [14, 15, 16]. Nevertheless the flow equation has the property of preserving the symmetries of the theory and, in addition, it has a quite simple and manageable structure. Moreover the PTRG flow, although it can not fully reproduce perturbative expansions beyond the one loop order [17], still does provide excellent results when used to evaluate the critical properties such as the critical exponents of the three dimensional scalar theories at the non-gaussian fixed point [18, 19]. In particular the determination is optimized when one takes the “sharp” limit of the cutoff function on the proper time and it turns out to be much more accurate than the one corresponding to a smoother regulator. The PTRG also provides excellent determinations of the energy levels of the quantum double well [20]. In fact, the use of the special type of PT regulator described in this paper and already discussed in [18, 20] realizes an localized integration over the “fast” variables at a given infrared running momentum k and, for this reason, it shows an impressive numerical convergence stability in the calculations of the critical exponents.

In this paper we shall instead be mainly concerned with the study of a a strong non-perturbative phenomenon like the SSB, for which the validity of PTRG equations has not been tested yet. In particular, the relevant question we would like to address in this paper is to analytically and numerically study the approach to the convexity for the EP obtained by means of a class of PTRG flow equations in the limit of vanishing infrared cutoff. A smeared type of proper-time regulator will be used which selects a localized integration in the “fast” variables in the path-integral. The resulting flow equation can

be thought of as an interpolation of a “smooth” modification of the LPA approximation of the Wegner-Houghton (WH) [13] “exact” flow equation, and the exponentially ultraviolet (UV) converging flow discussed in [14, 19]. It will be shown that the PTRGs can correctly describe the approach to convexity as $k \rightarrow 0$, and that give results which are completely consistent with the analysis performed in [5] for the WH equations, and in [4] for the “exact” evolution equation for the effective average action. The additional advantage is that below the upper critical dimension the PTRG flow equation predicts the expected discontinuity of the inverse compressibility, whereas the “exact” WH equation fails to do so.

In order to strengthen our analysis, we compare the result of our numerical investigation with the standard EP computed on a lattice by means of a Hybrid Monte Carlo approach. Our main conclusion is that lattice EP and PTRG flow equation agree extremely well even for relatively small lattices, both in the perturbative and non-perturbative regime.

2 Flow equations from proper-time regulators

Let us now review the basic assumptions in the derivation of the PTRG flow equation. We first calculate the wilsonian action in (1.2) in the one-loop approximation as

$$S_k^{1-loop}(\Phi) = -\frac{1}{2} \int_0^\infty \frac{ds}{s} f_k(s, \Lambda) \text{Tr} \left(e^{-s \frac{\delta^2 S_\Lambda}{\delta \varphi^2}} \Big|_{\varphi=\Phi} - e^{-s \frac{\delta^2 S_\Lambda}{\delta \varphi^2}} \Big|_{\varphi=0} \right) \quad (2.1)$$

where, following [21, 22, 23], we have introduced an heat-kernel smooth regulator f_k in the Schwinger proper time representation for the one-loop expression and we have subtracted the UV divergent contribution of a vanishing background field. The following prescription apply to the choice of f_k :

- $f_k(s=0, \Lambda) = 0$ in order to regularize the UV divergences as $s \rightarrow 0$
- $f_{k=0}(s \rightarrow \infty, \Lambda) = 1$ in order to leave the IR physics unchanged by the regulator
- $f_{k=\Lambda}(s, \Lambda) = 0$ in order to recover the original bare theory at the cutoff scale $k = \Lambda$.

The flow equation for the Wilsonian action S_k results from considering Eq.(2.1) in the infinitesimal momentum shell $k, k + \delta k$ and then *RG-improving the resulting expression*,

which amounts to substitute the bare action S_Λ with the running one $S_\Lambda \rightarrow S_k$ in the RHS of Eq.(2.1),

$$k \frac{\partial S_k(\Phi)}{\partial k} = -\frac{1}{2} \int_0^\infty \frac{ds}{s} k \frac{\partial f_k(s, \Lambda)}{\partial k} \text{Tr} \left(e^{-sS_k''(\Phi)} - e^{-sS_k''(0)} \right). \quad (2.2)$$

where primes indicate functional derivatives with respect to φ . At this point, one should stress that although the fast momentum integration in (2.1) has been obtained by assuming a trivial saddle point in the path-integral, the RG-improved flow equation (2.2) is instead a functional differential flow equation which is valid for a general average action $S_k(\Phi)$.

If we then project Eq.(2.2) onto its non-derivative part, the anomalous dimension η is set to zero, and the resulting flow equation for the local potential reads

$$k \frac{\partial U_k(\Phi)}{\partial k} = -\frac{K_d}{2} \int_0^\infty \frac{ds}{s^{1+d/2}} k \frac{\partial f_k(s, \Lambda)}{\partial k} \left(e^{-U_k''(\Phi)s} - e^{-U_k''(0)s} \right). \quad (2.3)$$

where $K_d = 2/(4\pi)^{d/2} \Gamma(d/2)$. For actual calculations we shall employ the following class of proper-time smearing functions

$$f_k^n(s, \Lambda) = \frac{\Gamma(n, sk^2) - \Gamma(n, s\Lambda^2)}{\Gamma(n)} \quad (2.4)$$

where $\Gamma(a, z) = \int_0^z dt t^{a-1} e^{-t}$ is the incomplete Gamma function and n a positive real number. Note that $\lim_{n \rightarrow \infty} f_k^n(n s, \Lambda) = \theta(s - k^2) - \theta(s - \Lambda^2)$.

Since $k \partial \Gamma(n, sk^2) / \partial k = -2(sk^2)^n e^{-sk^2}$ the s -integration in (2.3) can be explicitly performed, having at last

$$k \frac{\partial U_k(\Phi)}{\partial k} = -\frac{K_d}{2} k^d \ln \left(1 + \frac{U_k''(\Phi)}{k^2} \right) \quad n = \frac{d}{2} \quad (2.5)$$

$$k \frac{\partial U_k(\Phi)}{\partial k} = \frac{M_n^d}{(4\pi)^{d/2}} k^d \left(1 + \frac{U_k''(\Phi)}{nk^2} \right)^{d/2-n} \quad n > \frac{d}{2} \quad (2.6)$$

$$k \frac{\partial U_k(\Phi)}{\partial k} = \frac{1}{(4\pi)^{d/2}} k^d \exp \left(-\frac{U_k''(\Phi)}{k^2} \right) \quad n \rightarrow \infty \quad (2.7)$$

where $M_n^d = n^{d/2} \Gamma(n - d/2) / \Gamma(n)$, and in particular $M_\infty^d = 1$. In order to simplify the notation we have not explicitly written in the RHS of the equations the field independent contributions which correspond to a trivial shift of the vacuum energy at $k = 0$. Eq.(2.5)

is obtained from the $n = d/2$ limit by performing the trivial rescaling $k \rightarrow \sqrt{d/2}k$ of the infrared cutoff. It coincides with the LPA approximation of the “exact” WH sharp cut-off equation [22]. Eq.(2.6) converges to Eq.(2.7) as $n \rightarrow \infty$. In other words, the n -dependence in the cutoff interpolates between a WH type of equation and the “exponential” RG equation (2.7).

3 Analytical and numerical results

We shall now analytically and numerically study the RG flow below the critical line. Eq.(2.2) is in principle an evolution equation for a generic Wilsonian action $S_k(\Phi)$ and already in the simplest LPA approximation described in (2.5-2.7) it directly exhibits the approach to convexity as $k \rightarrow 0$. In other words, the non-perturbative features like spin waves, kinks or instantons are already included in Eq.(2.2). This result should not come entirely as a surprise since we already stressed that (2.5) obtained for $n = d/2$, is the LPA approximation of the “exact” Wegner-Houghton equation studied in [5]. In this respect, Eq.(2.6) and Eq.(2.7) can be thought of as smooth-cutoff modifications of the sharp cutoff WH equation, and it is then important to understand their IR behaviour below the critical temperature. In particular, the location of the polar singularity in Eq.(2.6) in the (Φ, k^2) plane seems to be n -dependent:

$$nk^2 + U_k''(\Phi) = 0 \tag{3.1}$$

so that in the limit $n \rightarrow \infty$, it becomes an essential singularity at $k = 0$ in Eq.(2.7). The relevant question, is to understand how the convexity of the free energy is recovered in the $k \rightarrow 0$ limit in these cases.

Our discussion will be mainly concerned with $n > d/2$, because the $n = d/2$ case has extensively discussed by [5] and the $n \rightarrow \infty$ case can be often extrapolated as a large n regime of (2.6). (numerically one does not see any relevant difference between (2.6) and (2.7) already for $n \sim 20$).

In order to study the behavior of the solution of Eq.(2.6) near $\Phi = 0$ it is convenient to introduce the rescaled potential and field

$$V_k = M_n^d / (4\pi)^{d/2} U_k \quad \phi = \sqrt{M_n^d / (4\pi)^{d/2}} \Phi. \tag{3.2}$$

It is then convenient to take the second derivative of Eq.(2.6) with respect to ϕ and to define a new variable $W_k(\phi)$ through

$$W_k(\phi) = \left(1 + \frac{V_k''}{nk^2}\right)^{d/2-n} \quad (3.3)$$

which becomes large and positive in the broken phase near $\phi = 0$ for $k \rightarrow 0$. In terms of this new variable Eq.(2.6) becomes

$$W_k'' = -2k^{-d+2}n\left(1 - W_k^{-\frac{1}{n-d/2}}\right) - \frac{nk^{-d+2}}{n-d/2} W_k^{-\frac{n+1-d/2}{n-d/2}} k \frac{\partial W_k}{\partial k} \quad (3.4)$$

and prime means now derivative wrt ϕ . In Eq.(3.4), when W_k is large and positive, we can neglect terms which are suppressed as inverse power of W_k and obtain the solution

$$W_k = n k^{-d+2}(\phi_0^2 - \phi^2) \quad (3.5)$$

with $|\phi| < \phi_0$, which is well behaved for any value of $k > 0$, being ϕ_0 an integration constant. Since our approach breaks down at $\phi = \phi_0$, we can thus identify ϕ_0 as the value of the field at the coexistence.

By inserting solution (3.5) back in (3.3) and solving for $U_k''(\Phi)$ we have the well-known behavior

$$U_k(\phi) = -\frac{nk^2}{2}\phi^2 + O(k^2\phi^2) \quad (3.6)$$

which is consistent with the analysis of [3, 4]. Incidentally, we note that (3.6) shows that the approach to the flat bottom is slower for larger values of n .

For the sake of completeness we notice that the $n \rightarrow \infty$ limit of (3.4) reads

$$W_k'' = 2k^{-d+2} \ln W_k - \frac{k^{-d+2}}{W_k} k \frac{\partial W_k}{\partial k} \quad (3.7)$$

while if we instead define $W_k(\phi) = \ln(1 + V_k''/k^2)$, Eq.(2.5) implies

$$W_k'' = 4k^{-d+2} - 2e^{W_k} k \frac{\partial W_k}{\partial k}. \quad (3.8)$$

Although no simple analytical solution is available in the broken phase near $\phi = 0$ for Eq.(3.7) we can still understand how the regulator affects the approach to the spinoidal line.

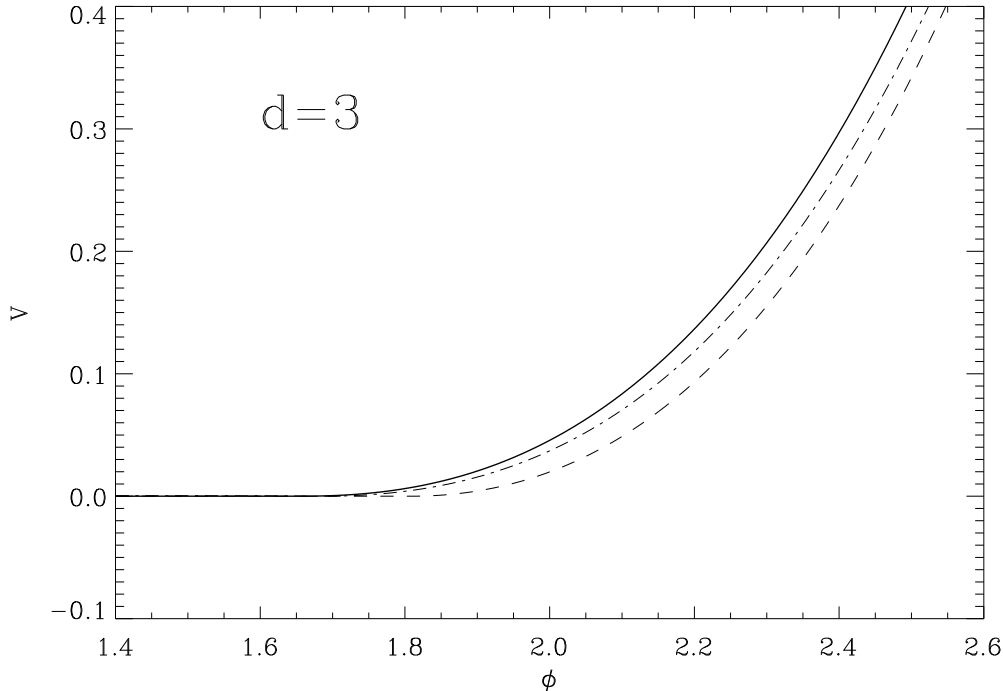


Figure 1: The blocked potential in $d = 3$. The solid line is for $n = 1.5$ (WH), the dashed is for $n = 2$ and the dot-dashed is for $n = 4$

In fact, when W_k is large and negative in Eq.(3.8), the diffusive term $\partial W/\partial k$ is exponentially suppressed in this case and we obtain Eq.(3.6) with $n = 1$ (see also [5]). On the contrary when W_k is large and positive in Eq.(3.4) and Eq.(3.7) the diffusive term is only power-law suppressed. In particular the suppression is the slowest for $n \rightarrow \infty$, like $1/W_k$, while if $n = d/2 + \epsilon$ (being ϵ small and positive), the suppression is like $W_k^{-(1+\epsilon)/\epsilon}$ and (3.5) is clearly reached faster as ϵ gets smaller. In other words convexity is best achieved with a small value of ϵ .

An important issue related with the above discussion is to understand how the inner solution joins the outer region $\phi > \phi_0$. For Eq.(2.5) it is known that a fixed point solution for $k \rightarrow 0$ is present, but it predicts a continuous second derivative of the effective potential for $d < 4$, which corresponds to a diverging compressibility at the transition (see [5] for an extended discussion on this point). The relevant question is whether the use of a

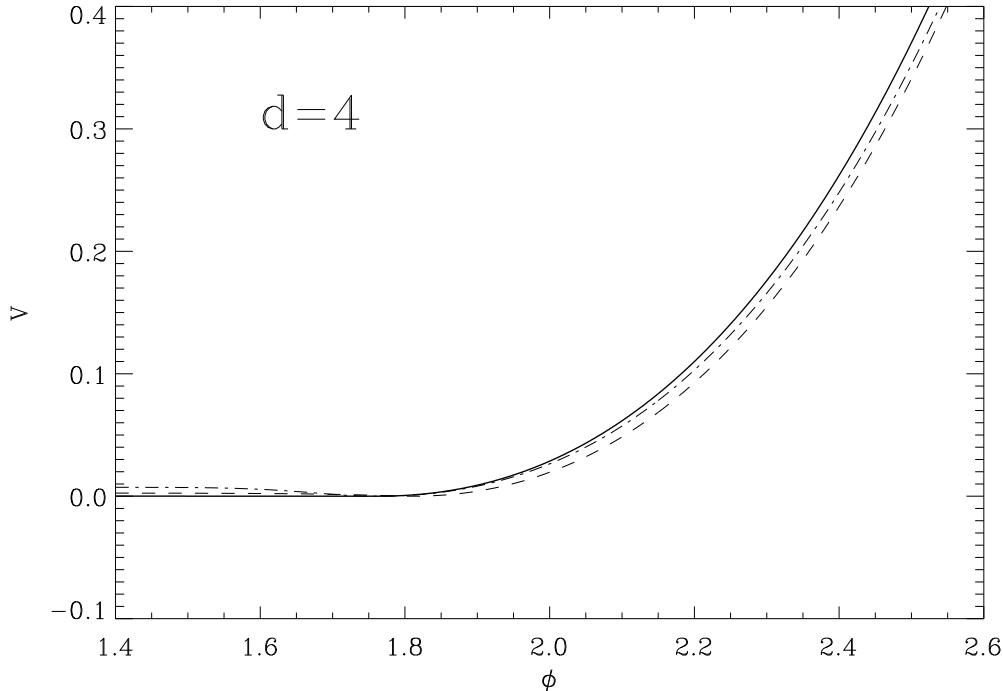


Figure 2: The blocked potential in $d = 4$. The solid line is for $n = 2$ (WH), the dashed is for $n = 3$ and the dot-dashed is for $n = 5$.

smooth cutoff regulator as Eq.(2.6) and Eq.(2.7) can cure this pathological behavior of the “exact” WH equation.

In order to investigate these problems in detail one must handle the problem numerically, by extracting an accurate numerical solution of the flow equation. We thus have solved Eq.(3.4) and Eq.(3.7) with the fully-implicit, predictor corrector finite-difference scheme described in [24] for which a rigorous result ensures convergence to the real solution for our numerical discretization grid.

Let us then write the bare potential as $V_\Lambda(\phi) = r_0\phi^2/2 + g_0\phi^4/4!$, and $|r_0| < 1$ being the bare mass measured in cutoff units. Fig.(1) and Fig.(2) show the blocked potential for $d = 3$, and $d = 4$, respectively, in the broken phase. As expected, if we push the integration closer to the $k \rightarrow 0$ limit all the curves approach a completely flat bottom as it is shown in Fig.(1) and Fig.(2) in $d = 3$ and $d = 4$, respectively, for various values of

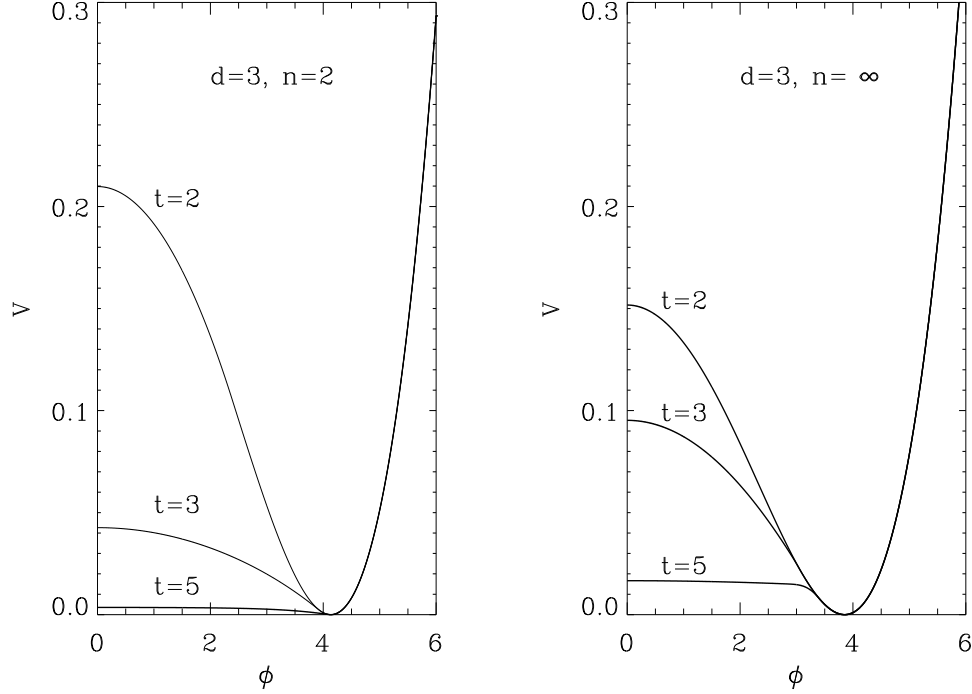


Figure 3: The blocked potential in $d = 3$ for various values of the RG time t .

n . In this case $r_0 = -0.6$, $g_0 = 1.0$, and the final value of the RG “time” is $t = -10$. Different values of r_0 and g_0 leads to qualitatively similar results in the sense that, as long as we are below the critical line, the flow always approaches the flat bottom convex potential.

As we discussed above, we also notice from Fig.(2) that the convergence to convexity is much faster for smaller values of n . A plot for different values of the RG time t is depicted in Fig.(3) where the expected behavior is discussed: as it is apparent from these plots the the potential for $n = 2$ is much closer to the flat and convex solution already for $t = 5$, than the $n = \infty$ case where, although a flat bottom is present near $\phi = 0$, convexity is not achieved yet. It is numerically difficult to reach higher values of t while keeping the mesh spacing constant if $n \rightarrow \infty$. We find that in order to reproduce the convexity at an acceptable level ($|\min(U) - U(0)| \sim 10^{-2}$ for $g_0 = O(1)$) the time step and the mesh spacing have to be both of the order of at least 10^{-3} , which is not very efficient from

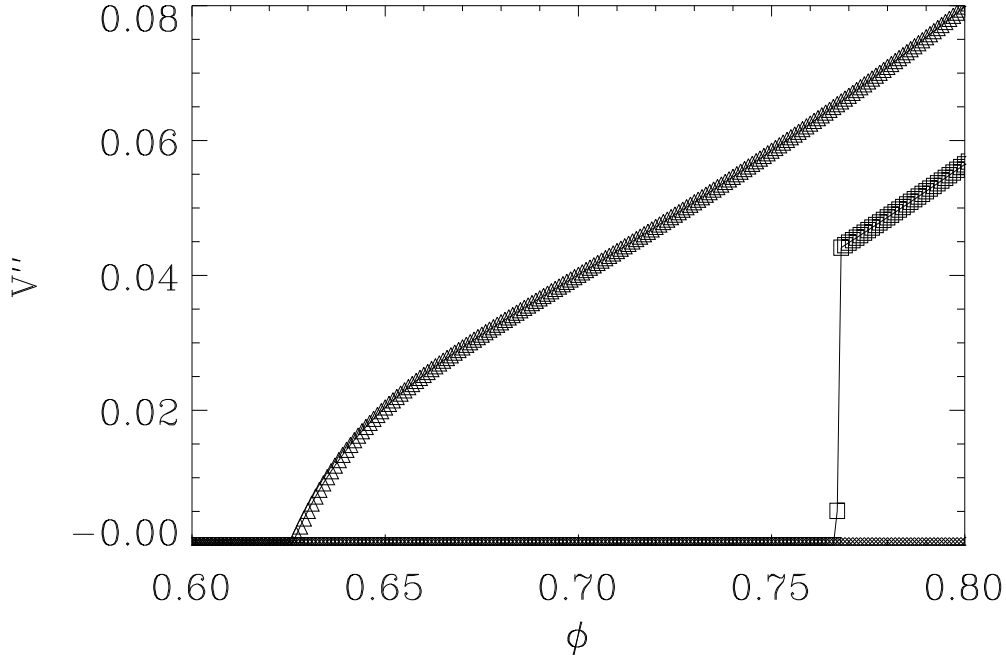


Figure 4: V'' as a function of ϕ in the broken phase for $d = 3$ and with $r_0 = -0.1$ and $g_0 = 1.2$. The squares are for $n = 3$ while the triangles are for the WH equation. The discontinuity is clearly visible in the first case, while it is not present for the WH equation.

the numerical point of view. On the contrary, if we choose $n = d/2 + \epsilon$ (ϵ positive and small), then $|\min(U) - U(0)| \sim 10^{-3}$ already with a mesh spacing one order of magnitude greater. Although we find numerical evidence that for $n \rightarrow \infty$ the solution approaches a flat bottom near the origin, we cannot exclude that convexity is never reached in this case.

An important result of our analysis is that the second derivative of the potential shows the expected discontinuity for $3 \leq d < 4$, for any $n > d/2$, as opposed to the “exact” WH equation, for which the spinoidal line merges with the coexistence line in $d = 3$. This is clearly shown in Fig.(4), where the discontinuity is visible in the numerical output because always only one grid point is present in the jump, and this feature does not depend on further refinements of the spatial grid. Similar behavior is also observed in $d = 3.5$, as it

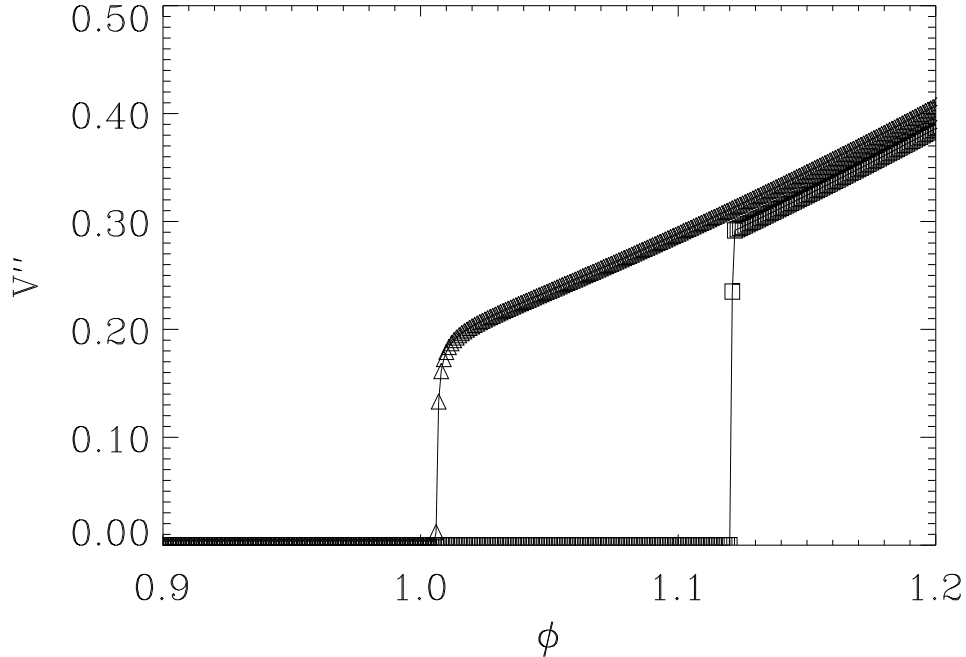


Figure 5: V'' as a function of ϕ in the broken phase for $d = 3.5$ and with $r_0 = -0.1$ and $g_0 = 1.2$. The squares are for $n = 3$ while the triangles are for the WH equation. The jump is clearly seen for the squares while there is a continuous transition for the WH equation

is apparent from Fig.(5).

4 Monte Carlo simulations

Monte Carlo simulations of the ϕ^4 model have been performed on $d = 2, 3, 4$ lattices in order to evaluate the Effective Potential and compare its determination with the numerical solution of the flow equations. In a lattice simulation, the inverse lattice spacing acts as an UV momentum cutoff, while the finite size introduces an IR cutoff. The model was discretised following the standard approach in [31], and the field configurations were generated with the Hybrid Monte Carlo algorithm. Introducing an uniform external current J , a discrete version of the action can be written as follows:

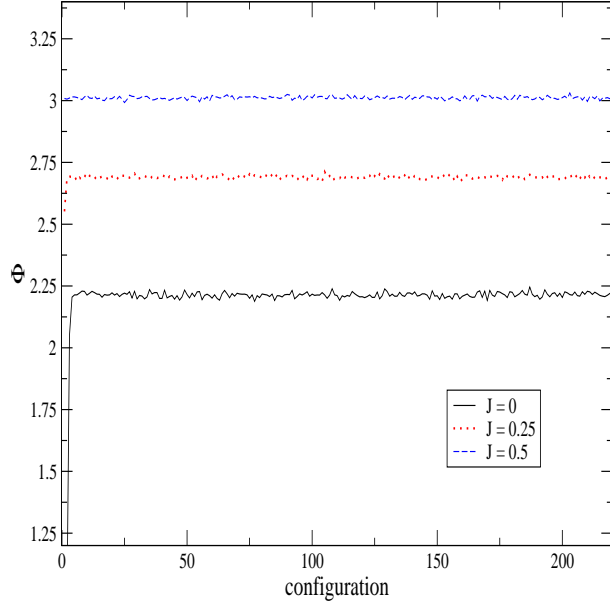


Figure 6: The average field as evaluated by the HMC simulation, in the $d = 3$ case ($L = 16$), with parameters $a^2 r_0 = -0.2$, $ag_0 = 0.24$. The results for three different values of J are shown.

$$S[\phi] = a^d \sum_n \left[\frac{1}{2a^2} \sum_{\mu=1}^d (\phi_{n+\mu} - \phi_n)^2 + V(\phi_n) - J\phi_n \right] \quad (4.1)$$

where n is the site index, a is the lattice spacing and

$$V(\phi) = a^2 \frac{r_0}{2} \phi^2 + a^{4-d} \frac{g_0}{4!} \phi^4 \quad (4.2)$$

Introducing the normalization $a^{d/2-1}\phi \rightarrow (2\kappa)^{1/2}\phi$ and $a^{d/2+1}(2\kappa)^{1/2}J \rightarrow J$, the discretised, dimensionless action is:

$$S[\phi] = \sum_n \left[-2\kappa \sum_{\mu=1}^d \phi_{n+\mu}\phi_n + \phi_n^2 + \lambda(\phi_n^2 - 1)^2 - \lambda - J\phi_n \right] \quad (4.3)$$

where

$$a^2 r_0 = \frac{1 - 2\lambda}{\kappa} - 2d \quad a^{4-d} g_0 = \frac{6\lambda}{\kappa^2} \quad (4.4)$$

Periodic boundary conditions have been assumed. Both cold and hot starts have been tested, and once thermalization was achieved, the average of the field over the entire

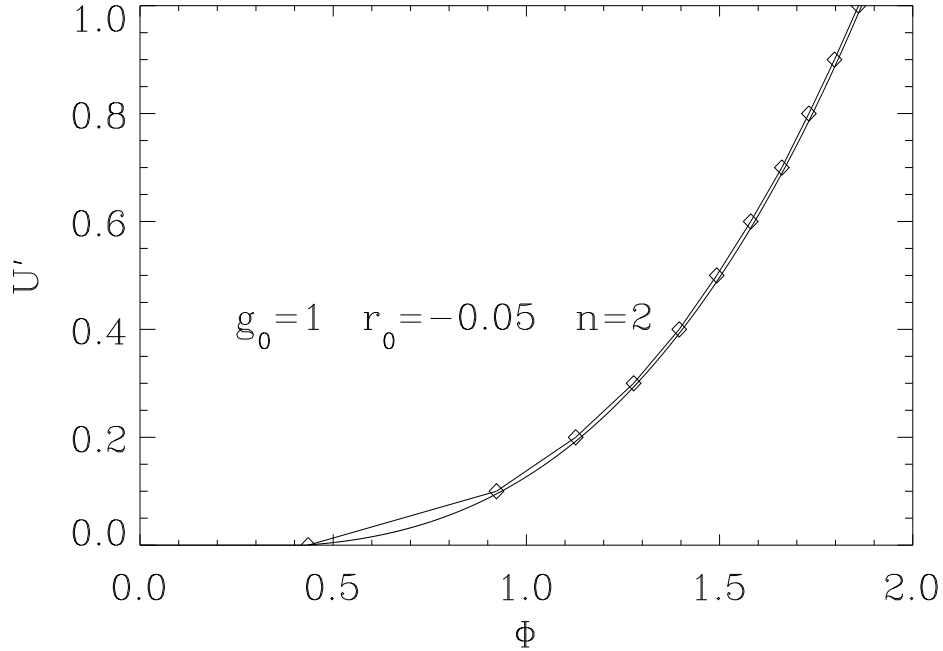


Figure 7: The blocked potential from the flow equation in $d = 3$ vs the MC simulation for a volume of 12^3 in the weak coupling case (MC errors negligible on this scale).

lattice was computed on each configuration:

$$\Phi = \frac{1}{L^d} \sum_n \phi_n \quad (4.5)$$

where L is the number of lattice sites in each direction. The results were saved every 50 configurations to decorrelate the results. In each case, 200 uncorrelated configurations were collected in order to get a statistically accurate determination of the average field. It should be noticed that the size of the statistical fluctuations decreased as the external current J was increased, as expected. In all cases, statistical errors have been estimated using the bootstrap technique (1000 samples) and found to be negligible. Simulations have been run with different lattice volumes, and finite size effects have been found to be negligible. For each choice of the numerical parameters (κ, λ) , the simulation was run with several values of the external current J . This procedure was not very different from

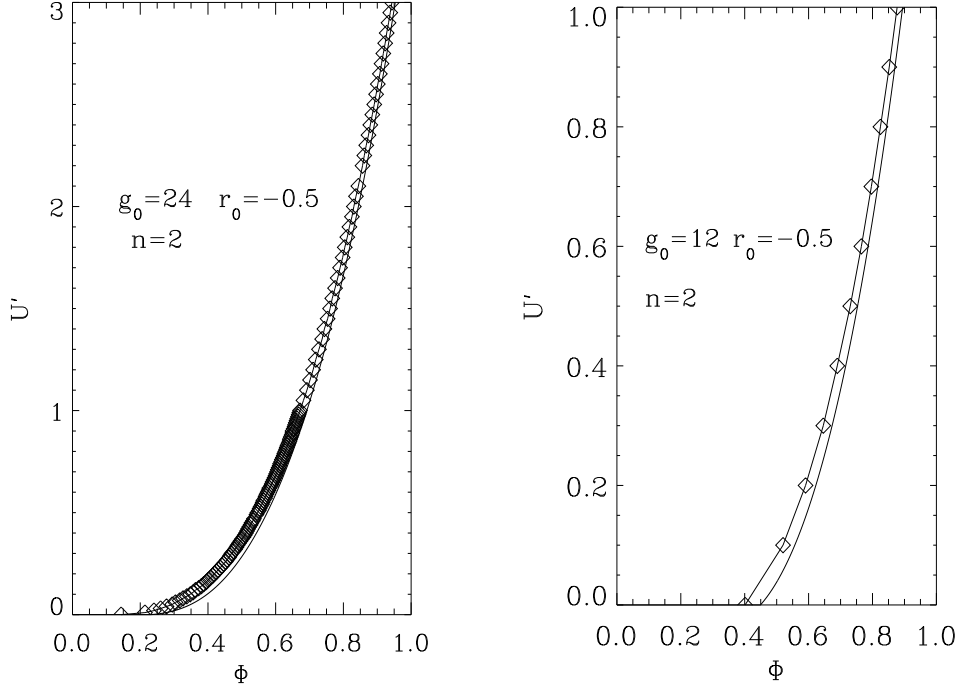


Figure 8: The blocked potential from the flow equation in $d = 3$ vs the MC simulation for a volume of 12^3 in the strong coupling case (MC error bars invisible on this scale).

that sketched in [32]. The relation $\Phi(J)$ was then inverted to get $J(\Phi)$, and thus the first derivative of the Effective Potential by

$$J = U'(\Phi) \tag{4.6}$$

We would like to compare U' as computed from (4.6) with the same quantity obtained by numerical integration of the flow equation. Although it would be possible to compare the constraint effective potential [33] at a given scale $k \propto 1/\Omega$, with the blocked potential as computed from the flow equation at a scale k , it is more interesting to focus on the $k \rightarrow 0$ limit, where possible non-universal features due to the regulator may disappear. As we discussed in the introduction we prefer to use the external current method because it is simpler to implement and as accurate as the constraint effective potential method [32].

We explore a set of parameters which is not close to the critical line, so that finite-size effects can be neglected, and we are able to compare the result of the flow equation directly to the lattice determination of the effective potential. In particular we find that it is not necessary to construct a lattice version of the RG flow equation as discussed in [34]. We have integrated Eq.(3.4) rewriting all the relevant quantities in units of the UV cut-off and then we have followed the evolution down to $t \rightarrow \infty$ with the help of the numerical integrator. In order to show the predictive power of our approach we have not fine-tuned the bare parameters in the RG flow equations to reproduce renormalized mass and coupling constant obtained in the lattice calculation as done in [34]. Instead, we have decided to set the same bare mass and coupling constant in the lattice bare potential (4.2) and in the bare potential of the RG equation. Moreover we have rescaled back our potential and field according to (3.2) so that we get $U'_{k=0}(\Phi)$ out of the numerical computation. According to the analysis of the previous session we have considered $n \in (d/2, d]$ where the numerical stability is best achieved.

The results are shown in Fig.(7) and Fig.(8) for $n = 2$ and $d = 3$, where it is apparent that there is already a very good agreement with the MC data both in the weak and in the strong coupling regime. Better agreement could probably be achieved by including the wave-function renormalization function, but this is not our main concern in this investigation.

5 Conclusions

We have discussed the PTRG flow equation below the critical line in a scalar theory. In particular we have shown that the convexity property of the free energy is recovered by integration of the LPA flow equation in the $k \rightarrow \infty$ limit. Within a class of n -dependent proper time regulator, the approach to the correct flat bottom potential is faster when $n = d/2 + \epsilon$ being ϵ positive and small. The expected discontinuity of the U'' at the transition is correctly reproduced for any value of $\epsilon > 0$ as opposed to the “exact” WH

flow ($\epsilon = 0$), which does not show this feature. We have performed an extensive MC investigation of the EP in $d = 3$ in order to discuss the numerical predictions and we found very good agreement both the strong coupling and weak coupling phase without resorting to a fine-tuning procedure between the bare parameters in the MC and in the RG flow equation. We anticipate that our result can be relevant in gauge theory where the presence of the PT regulator is an essential tool deriving a non-perturbative flow equation [23].

Acknowledgements

We acknowledge Martin Reuter and Dario Zappalá for useful comments. G. Lacagnina acknowledges the financial support by the DFG-Forschergruppe “Lattice Hadron Phenomenology” and wishes to thank V. Braun, A. Schäfer and M. Göckeler for useful discussions.

References

- [1] P.C. Hemmer, J.L. Lebowitz, in *Phase Transitions and Critical Phenomena*, edited by C. Domb and M.S.Green (Academic, New York, 1976), Vol 5b.
- [2] E.J. Weinberg, Ai-qun Wu, Phys. Rev. **D36** (1987), 2474.
- [3] A. Ringwald, C. Wetterich, Nucl. Phys. **B353** (1991), 303.
- [4] N.Tetradis, C. Wetterich, Nucl. Phys. **B383** (1992), 197.
- [5] A. Parola, D. Pini, L. Reatto, Phys. Rev. **E48** (1993), 3321; A. Parola, L. Reatto, Phys. Rev. Lett. **53** (1984), 2417; Phys. Rev. **A31** (1985), 3309; Adv. in Phys. **44** (1995), 211; J. Phys. Cond. Matter **8** (1996), 9221.

- [6] J. Berges, N. Tetradis, C. Wetterich, Phys. Rep. **363** (2002), 223 and hep-ph/0005122.
- [7] J. Alexandre, V. Branchina, J. Polonyi, Phys. Lett. **B445** (1999), 351.
- [8] L. O’Raifeartaigh, A. Wipf, H. Yoneyama, Nucl. Phys. **B271** (1986), 273.
- [9] K.G. Wilson, M.E. Fisher, Phys. Rev. Lett. **28** (1972), 240; K.G. Wilson, J. Kogut, Phys. Rep. **12C** (1974), 75.
- [10] G. Papp, B.J. Schäfer, H.J. Pirner, J. Wambach, Phys. Rev. **D61** (2000), 096002.
- [11] B.J. Schäfer, H.J. Pirner, Nucl. Phys. **A627** (1997), 481; Nucl. Phys. **A660** (1999), 439; J. Meyer, G. Papp, H.J. Pirner, T. Kunihiro, Phys. Rev. **C61** (2000), 035202.
- [12] O. Bohr, B.J. Schäfer, J. Wambach, *Renormalization group flow equations and the phase transition in $O(N)$ models*, Preprint July 2000, and hep-ph/0007098.
- [13] F. J. Wegner, A. Houghton, Phys. Rev **A8** (1972) , 401.
- [14] D. F. Litim, Phys. Rev. **D 64** (2001) , 105007; JHEP, 0111, 059, (2001).
- [15] D. F. Litim, J. M. Pawłowski, Phys. Lett. **B 516** (2001), 197.
- [16] D. F. Litim, J. M. Pawłowski, Phys. Rev. **D 65** (2002), 081701(R); Phys. Rev. **D 66** (2002), 025030; Phys. Lett. **B 546** (2002), 279.
- [17] D. Zappalà, Phys. Rev. **D 66** (2002), 105020.
- [18] A. Bonanno, D. Zappalà, Phys. Lett. **B504** (2001), 181.
- [19] M. Mazza, D. Zappalà, Phys. Rev. **D 64** (2001), 105013.
- [20] D. Zappalà, Phys. Lett. **A 290** (2001), 35.
- [21] M. Oleszczuk, Z. Phys. **C64**, (1994), 533.

- [22] S.-B. Liao, Phys. Rev. **D53**, (1996), 2020.
- [23] S.-B. Liao, Phys. Rev. **D56**, (1997), 5008.
- [24] W.F. Ames, *Numerical methods for Partial Differential Equations* (Academic, London, 1977).
- [25] J. Zinn-Justin, *Quantum Field Theory and Critical Phenomena*, (3rd ed., Oxford University Press, 1996).
- [26] P. Butera, M. Comi, Phys. Rev. **B56** (1997), 8212.
- [27] B.G. Nickel, J.J. Rehr, J. Stat. Phys. **61** (1990), 1.
- [28] C.F. Baillie, R. Gupta, K.A. Hawick, G.S. Pawley, Phys. Rev. **B45** (1992), 10438, and references therein.
- [29] H.G. Ballesteros, L.A. Fernandez, V. Martin-Mayor, A. Munoz Sudupe, Phys. Lett. **B387** (1996), 125.
- [30] M. Hasenbush, J. Phys. **A32** (1999), 4851.
- [31] I. Montvay, G. Münster, *Quantum Fields on a Lattice*, (Cambridge University Press, 1994).
- [32] A. Ardekani, A.G. Williams, Phys. Rev. E **57** (1998), 6140.
- [33] O’Raifeartaigh, A. Wipf, H. Yoneyama Nucl. Phys. **B 271** (1986), 653.
- [34] J.R. Shepard, V. Dmitrasinovic, Phys. Rev. **D51** (1995), 7017.